Distinct Membrane Binding Properties of the Two Non-visual Arrestins

Thomas D. Killeen[1*], Katelyn Tepper[2*], Kyle W. Miller[2*], Yasmin Aydin[2*], Ya Zhuo[3*], Shuaitong Zhao[2], Jason M. Conley[2], Rachel Tat[4], Candice S. Klug[5], Adriano Marchese[3], Valerică Raicu[1#], Qiuyan Chen[2#]

[1] Department of Physics, University of Wisconsin-Milwaukee; Milwaukee WI 53211, USA.
[2] Department of Biochemistry and Molecular Biology, Indiana University School of Medicine; Indianapolis, IN 46202, USA.
[3] Department of Biochemistry, Medical College of Wisconsin, Milwaukee WI 53211, USA.
[4] Department of Microbiology and Immunology, Indiana University School of Medicine; Indianapolis, IN 46202, USA.
[5] Department of Biophysics, Medical College of Wisconsin, Milwaukee WI 53211, USA.

* These authors contributed equally.
# Corresponding authors. Email: vraicu@uwm.edu, qch2@iu.edu.

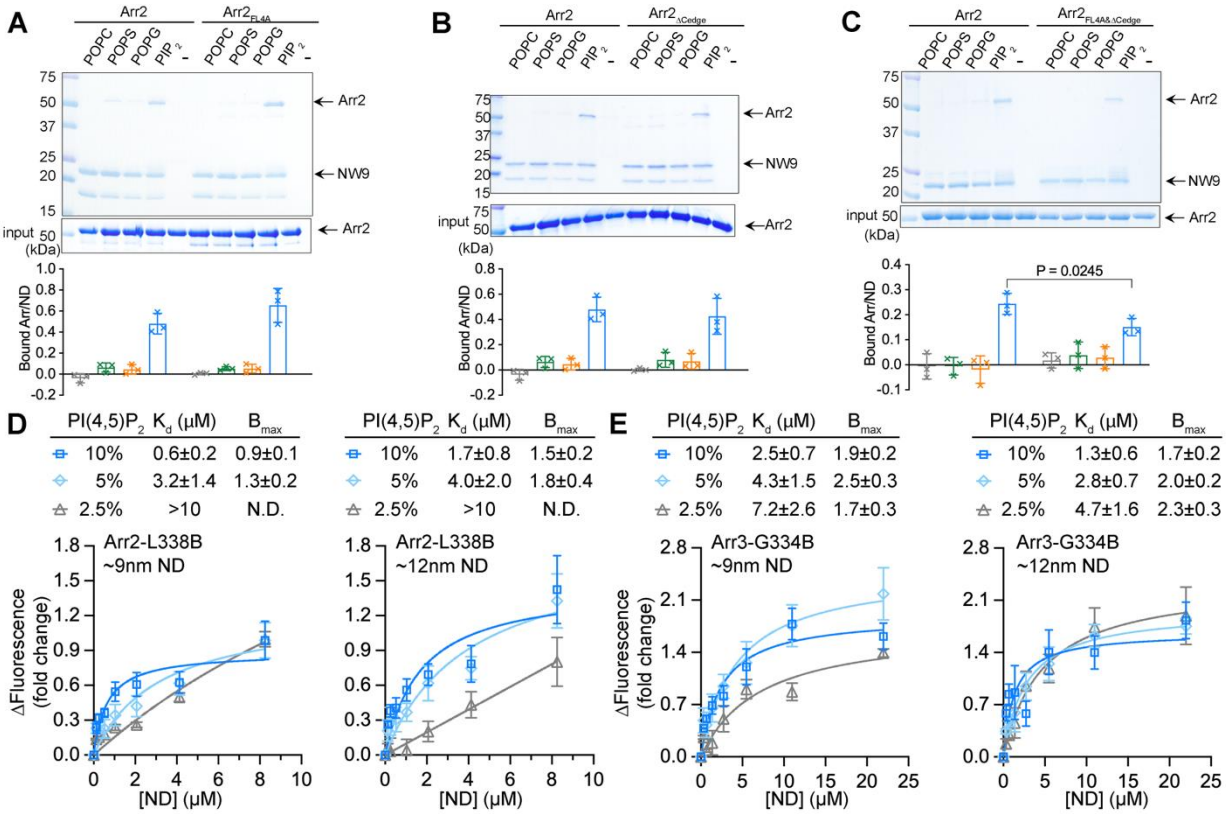

Supplementary Figure 1. Arr2 utilizes multiple structural elements for membrane binding and the effects of nanodiscs size and PI(4,5)P_2 concentration on Arr2 and Arr3 interaction with nanodiscs. **A-C.** His-pulldown assays show that neither the finger loop mutation (Arr2$_{FL4A}$: L68A, V70A, L71A, L73A) (**A**) nor the C-edge deletion (Arr2$_{\Delta Cedge}$: Δ334-LLGDLASS-341) (**B**) alone affects Arr2 binding to PI(4,5)P_2 nanodiscs. Combining them (Arr2$_{FL4A\&\Delta Cedge}$) reduced Arr2 binding by ~40% (**C**). The ratio of bound arrestin band density to NW9 band density was plotted and compared using one-way ANOVA, followed by a Tukey multiple comparison test. Error bars represent S.D. from three technical replicates. **D, E.** Binding curves of Arr2-L338B (**D**) and Arr3-G334B (**E**) to ~9nm or ~12nm nanodiscs containing 2.5%, 5%, or 10% PI(4,5)P_2 based on fluorescence changes in response to increasing nanodisc concentration. The curves were fit with a one-site binding model in Prism to derive the K_d and B_{max} values.

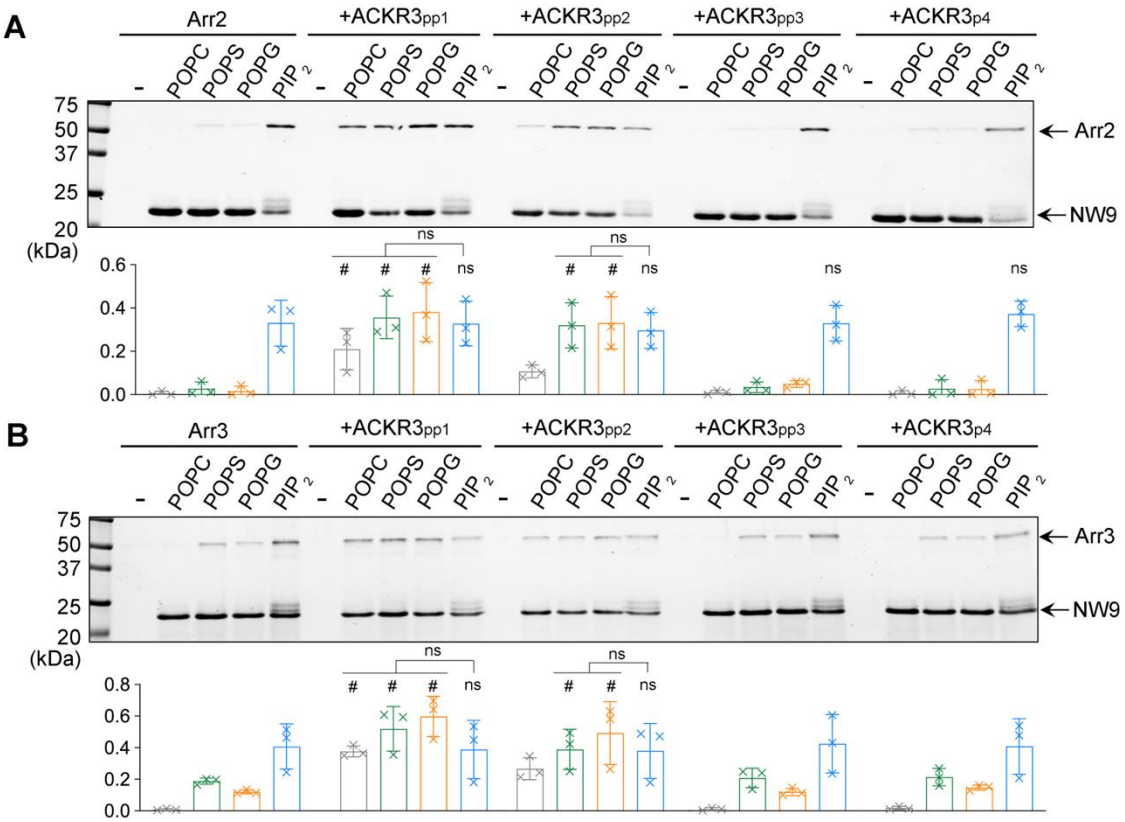

Supplementary Figure 2. Membrane tethered phosphopeptides anchor Arr2/3 at the membrane. A, B A HIS pulldown assay shows that ACKR3$_{pp1}$ and ACKR$_{pp2}$, but not ACKR3$_{pp3}$ and ACKR$_{p4}$, promote Arr2 (**A**) and Arr3 (**B**) binding to the POPS, POPG nanodiscs at levels similar to those observed with the PI(4,5)P_2 nanodiscs. The ratio of bound arrestin band density to NW9 band density was plotted and compared using two-way ANOVA, followed by a Tukey multiple comparison test, within the Arr2 and Arr3 group, respectively. Error bars represent S.D. from three technical replicates. ns, not significant. # indicates $p<0.0001$, comparing nanodisc binding to a control without peptide within the same nanodisc group. Part of the same gel including Arr2/3 alone or in the presence of ACKR3$_{pp1}$ and ACKR$_{pp2}$ has been shown in Fig. 5A and B.

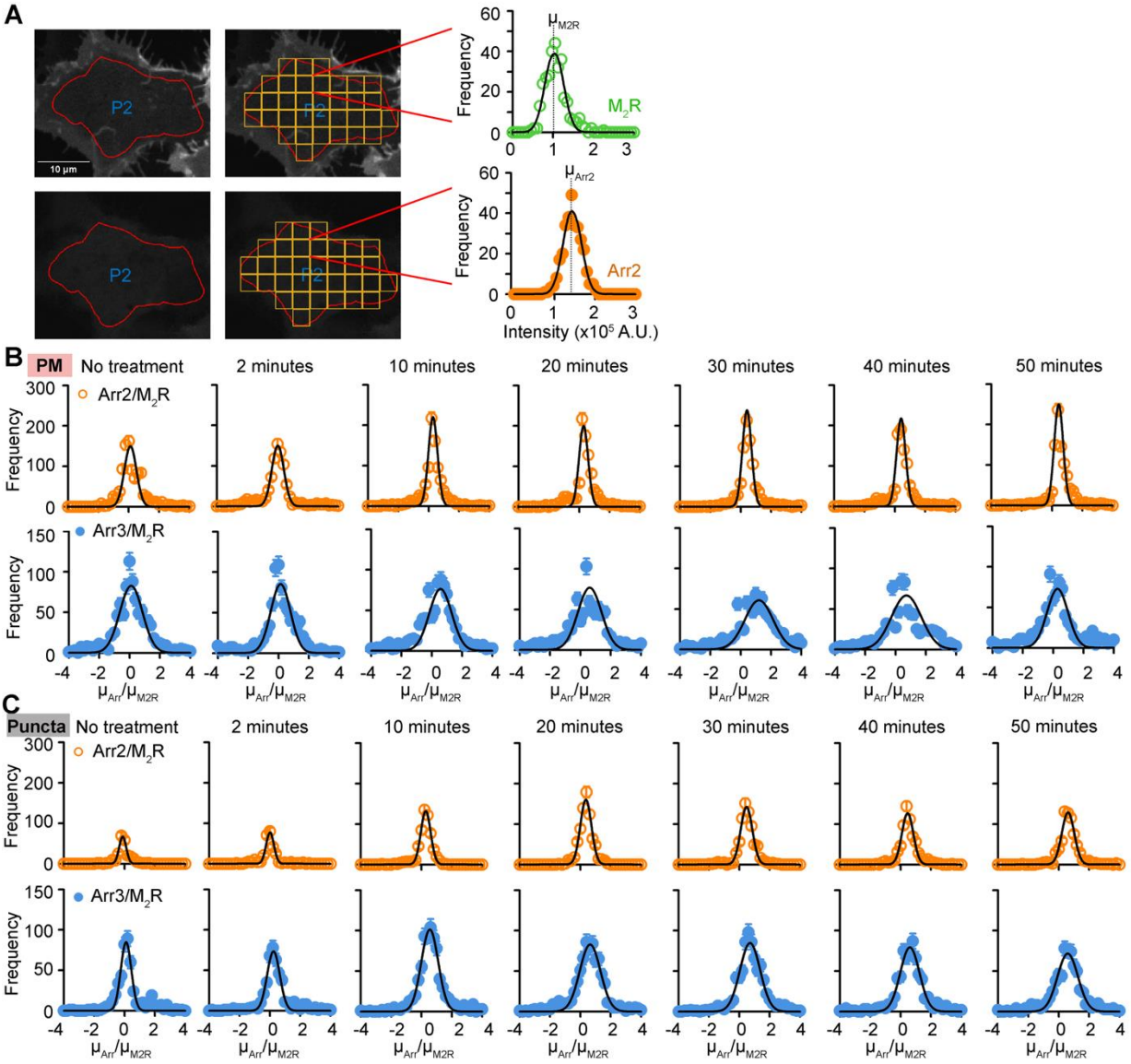

Supplementary Figure 3. FIF analysis of Arr2/3 and M_2R at the plasma membrane and within the CCPs before and after stimulation. A. ROIs were drawn using a polygon overlay tool (red outline), and each ROI was segmented into subsections (yellow boxes). Fluorescence intensities of M_2R and Arr2 at each pixel were used to generate histograms for each segment, which were fitted with a Gaussian function. The mean and standard deviation of each the Gaussian curve was used to compute Arr2-to-M_2R ratio for each segment in an image. This ratio computed from 300-500 segments were used to assemble histograms of Arr2-to-M_2R ratios at each time point, which are shown in panel B. The process was repeated for samples co-expressing Arr3 and M_2R. **B, C**. Distributions of Arr2/3-to-M_2R concentration ratios at selected time points from uniform membrane (**B**) and CCP (**C**) analysis. The errors are the square root of the frequency of occurrence of each ROI segment. The histograms were fitted with a Gaussian to determine the mean of concentration ratios, $\mu_{Arr2/M2R}$ and $\mu_{Arr3/M2R}$.

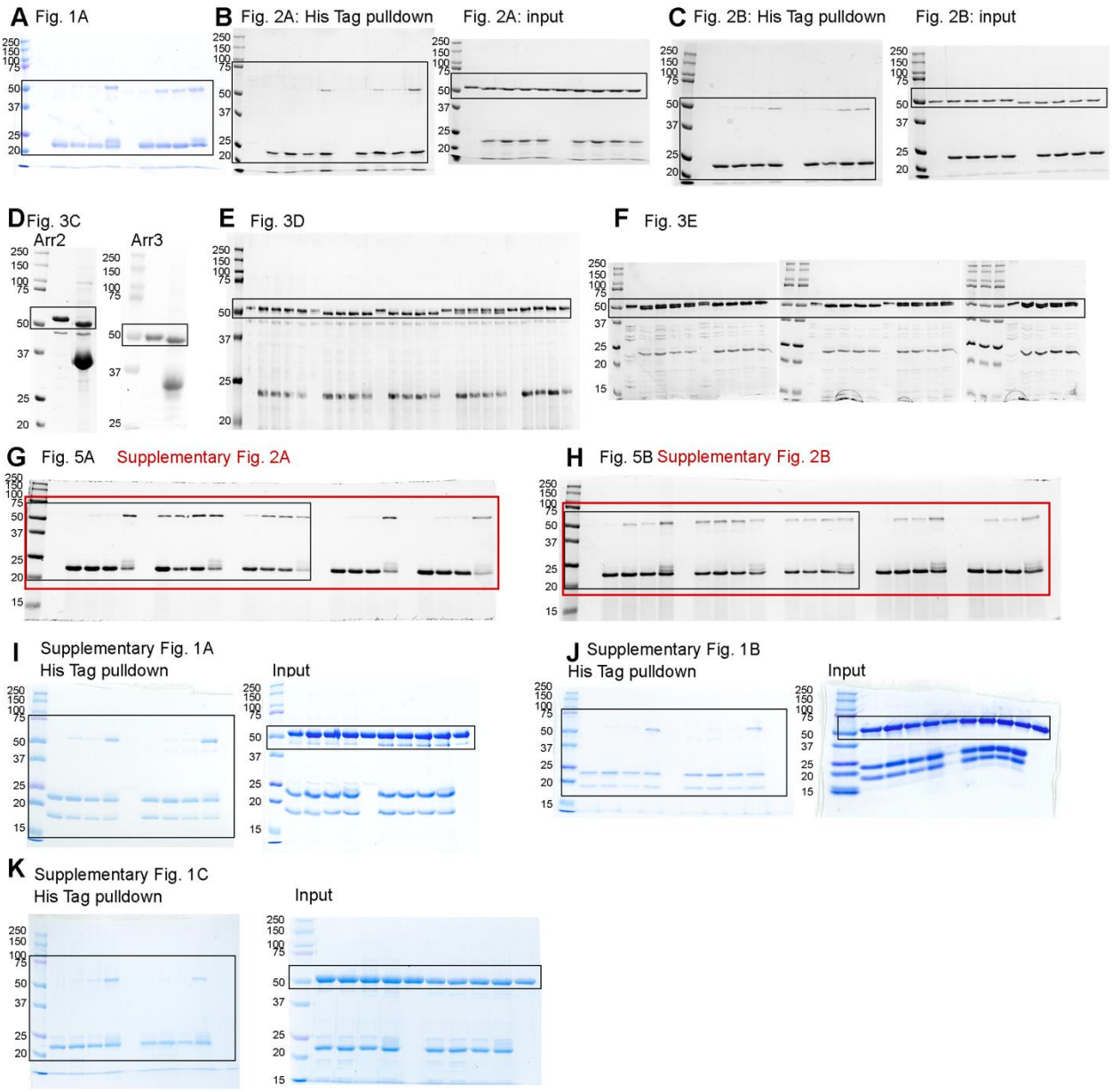

Supplementary Figure 4. Uncropped gels. Uncropped gels corresponding to Fig. 1A (A), Fig. 2A (B), Fig. 2B (C), Fig. 3C (D), Fig. 3D (E), Fig. 3E (F), Fig. 5A (G, black rectangular), Supplementary Fig. 2A (G, red rectangular), Fig. 5B (H, black rectangle), Supplementary Fig. 2B (H, red rectangle), Supplementary Fig. 1A (I), Supplementary Fig. 1B (J), and Supplementary Fig. 1C (K). Rectangles indicate the cropped areas in the figures.